

A QUASIPERIODIC MATHIEU EQUATION

RICHARD RAND

*Department of Theoretical and Applied Mechanics, Cornell University
Ithaca, NY 14853*

RANDOLPH ZOUNES and RACHEL HASTINGS

*Center for Applied Mathematics, Cornell University
Ithaca, NY 14853*

ABSTRACT

In this work we investigate the quasiperiodic Mathieu equation,

$$\ddot{x} + (\delta + \epsilon \cos t + \epsilon \cos \omega t) x = 0.$$

We use numerical integration, Lyapunov exponents, and a variety of perturbation methods to determine regions of stability in the δ - ω plane for fixed ϵ .

1. Introduction

Mathieu's equation [7],

$$\ddot{x} + (\delta + \epsilon \cos t) x = 0, \tag{1}$$

is the paradigm for problems in parametric excitation in which an autonomous linear structure is driven by a periodic forcer, usually in a direction perpendicular to the direction of motion (e.g., the vertically forced pendulum, dynamic buckling of an elastic column, water waves in a vertically driven channel).

This work concerns a natural extension of such problems to cases in which the forcer is quasiperiodic. We investigate the quasiperiodic (QP) Mathieu equation,

$$\ddot{x} + (\delta + \epsilon \cos t + \epsilon \cos \omega t) x = 0. \tag{2}$$

For a given set of parameters $(\delta, \omega, \epsilon)$, eq.(2) is said to be **stable** if all solutions are bounded, and **unstable** otherwise. We use numerical integration and Lyapunov exponents to determine regions of stability in the δ - ω plane for fixed ϵ . In addition, we obtain approximate analytic expressions for the transition curves bounding regions of stability using two distinct methods: regular perturbations and harmonic balance [9], [10]. Finally, we use singular perturbations to study the stability of eq.(2) for small ω and ϵ when δ is close to $\frac{1}{4}$ [6].

Eq.(2) has been investigated by perturbation methods in [1], [3], [8]. These authors have noted the failure of perturbations for small ϵ when ω takes on resonant values due to small-divisors. We shall show how the method of harmonic balance can be used to avoid these difficulties.

2. Numerical Integration

In order to obtain an approximate stability chart, we numerically integrated eq.(2) forward in time from arbitrarily chosen initial conditions at $t = 0$ up to $t = 20,000$. At each step we computed the amplitude $\sqrt{x(t)^2 + \dot{x}(t)^2}$ and judged a motion to be unstable if its amplitude became greater than a million times its initial value for any t between 0 and 20,000, and stable otherwise. Our results are displayed in Fig.1.

We note that the structure of the stability regions for the QP Mathieu equation is much more complicated than for the Mathieu equation [7].

3. Lyapunov Exponents

Lyapunov exponents [6] provide a second approach based on numerical integration with which we can obtain an approximate stability chart for eq.(2). The *Lyapunov exponent* of the solution $x(t)$ is defined as the following limit:

$$\lambda = \limsup_{t \rightarrow \infty} \frac{1}{t} \ln |x(t)|. \quad (3)$$

A positive Lyapunov exponent, $\lambda > 0$, corresponds to an unstable solution, and since there is no dissipation in eq.(2), stable solutions correspond to $\lambda = 0$. After numerically integrating eq.(2), we found it difficult to distinguish between small positive Lyapunov exponents and those which were truly zero. We resolved this by noting that Lyapunov exponents which are genuinely nonzero should maintain their values as the time of integration is increased. On the other hand, Lyapunov exponents that are genuinely zero will have computed approximations that tend to zero as the time of integration is increased. Our results are displayed as a contour plot in Fig.2.

4. Regular Perturbations

In the case of Mathieu's equation, regular perturbations have been used to provide approximate analytic expressions for the transition curves in the δ - ϵ plane which separate regions of stability from regions of instability [7]. The procedure, which is valid for small values of ϵ , is based on the result from Floquet theory that along a transition curve, there exist solutions with period 2π or 4π . This leads to the conclusion that when $\epsilon = 0$, regions of instability ("Arnold tongues") emanate from the δ axis at points given by

$$\delta = \delta_0 = \frac{n^2}{4}, \quad n = 1, 2, 3, \dots \quad (4)$$

Thus in the case of Mathieu's equation, we set

$$\delta = \delta_0 + \epsilon \delta_1 + \epsilon^2 \delta_2 + \dots \quad (5)$$

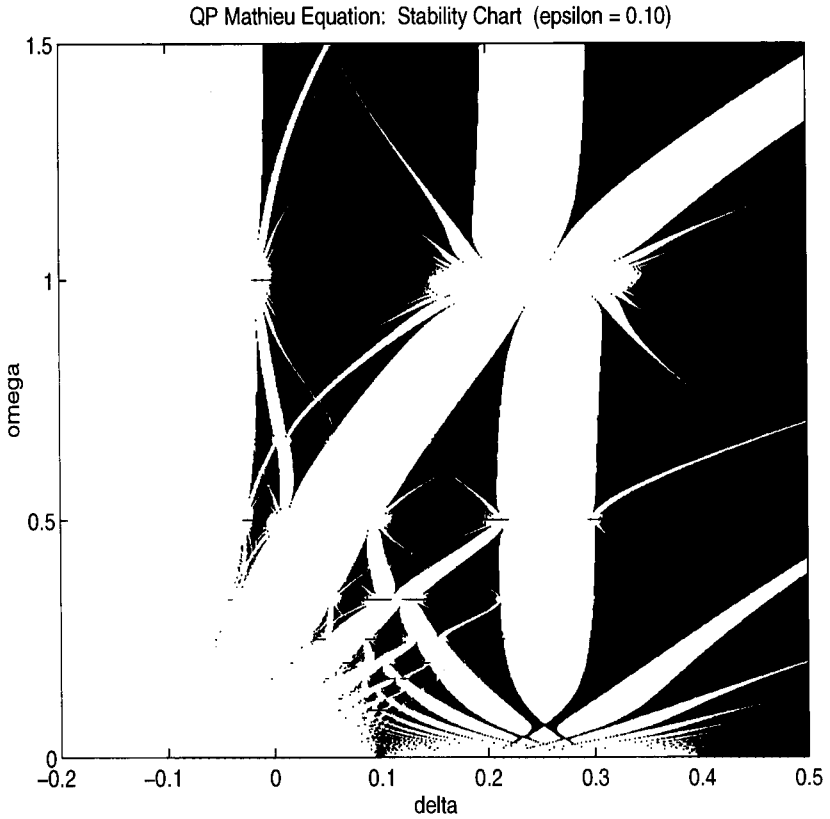


Fig.1. Stability of eq.(2) as determined directly from numerical integration. Points (δ, ω) in the blackened regions of the δ - ω parameter plane correspond to stable (bounded) solutions. $\epsilon = 0.1$.

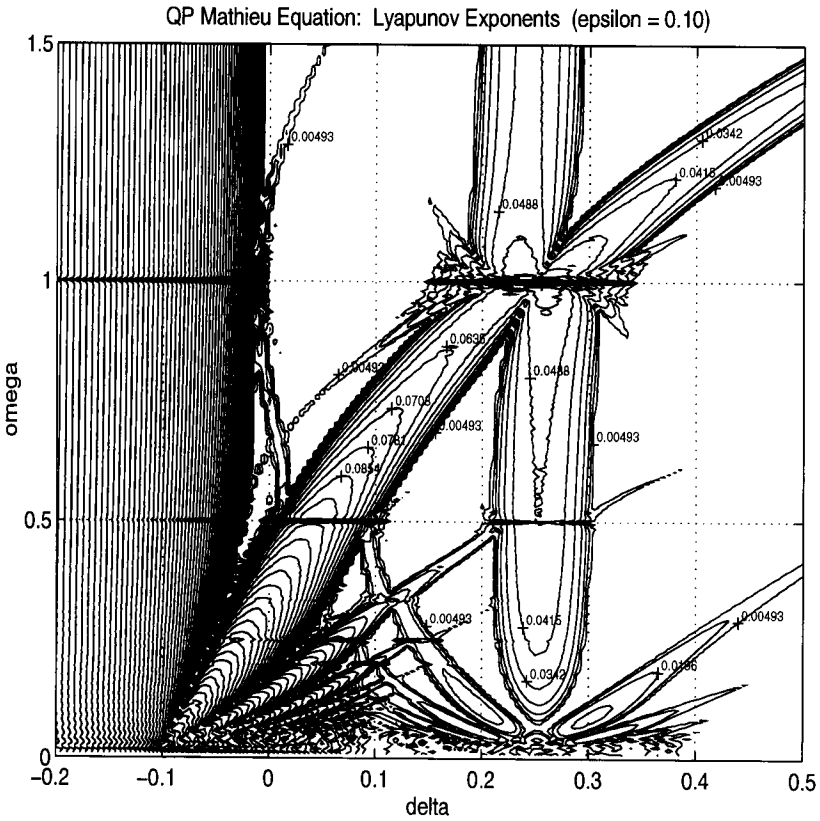


Fig.2. Contour plot of Lyapunov exponents. The level curves correspond to constant values of $\lambda > 0$ for which eq.(2) is unstable. $\epsilon = 0.1$.

$$x(t) = x_0(t) + \epsilon x_1(t) + \epsilon^2 x_2(t) + \dots \tag{6}$$

where $x_0(t)$ is separately equated to $\sin nt/2$ and $\cos nt/2$, and together with eq.(4), each yields a transition curve. The pair of curves associated with a given value of n yields an approximation to the corresponding Arnold tongue. (In the case of $n = 0$, however, a single transition curve occurs corresponding to $x_0(t) = 1$.) After substituting these power series expansions into Mathieu's equation, the coefficient δ_i is obtained by eliminating secular terms from the differential equation for $x_i(t)$.

We shall apply a similar scheme to the QP Mathieu equation. The key ansatz is the generalization of the transition points of eq.(4) to

$$\delta_0 = \frac{(n + m\omega)^2}{4}, \quad n = 0, 1, 2, \dots, \quad m = 0, \pm 1, \pm 2, \dots \tag{7}$$

The expansions (5), (6) are substituted into the QP Mathieu equation where $x_0(t)$ is separately equated to $\sin(\frac{n+m\omega}{2}t)$ and $\cos(\frac{n+m\omega}{2}t)$, and together with eq.(7), each yields a transition curve. Once again, the coefficient δ_i is obtained by eliminating secular terms from the differential equation for $x_i(t)$.

As an example of the kind of results obtained under this method (using computer algebra), take the cases $(n, m) = (1, 1)$ and $(1, -1)$:

Case $\delta_0 = \frac{1}{4}(1 + \omega)^2$: $n = 1$ and $m = 1$

$$\delta = \frac{1}{4}(\omega + 1)^2 - \frac{1}{2} \frac{\epsilon^2 (\omega^2 + \omega + 1)}{\omega (2\omega + 1)(\omega + 2)} + O(\epsilon^4) \tag{8}$$

$$\delta = \frac{1}{4}(\omega + 1)^2 + \frac{3}{2} \frac{\epsilon^2 (\omega^2 + 3\omega + 1)}{\omega (2\omega + 1)(\omega + 2)} + O(\epsilon^4) \tag{9}$$

Case $\delta_0 = \frac{1}{4}(1 - \omega)^2$: $n = 1$ and $m = -1$

$$\delta = \frac{1}{4}(1 - \omega)^2 + \frac{1}{2} \frac{\epsilon^2 (\omega^2 - \omega + 1)}{\omega (2\omega - 1)(\omega - 2)} + O(\epsilon^4) \tag{10}$$

$$\delta = \frac{1}{4}(1 - \omega)^2 - \frac{3}{2} \frac{\epsilon^2 (\omega^2 - 3\omega + 1)}{\omega (2\omega - 1)(\omega - 2)} + O(\epsilon^4) \tag{11}$$

Plots of transition curves generated under this method for $n = 0, 1, 2$ and $m = 0, \pm 1, \pm 2$, all valid to $O(\epsilon^4)$, are displayed in Fig.3. Note that the expressions for the transition curves are not valid in neighborhoods of $\omega = 0, \frac{1}{3}, \frac{1}{2}, \frac{2}{3}, 1, \frac{3}{2}, 2$, and 3 since there are terms that have vanishing denominators at these resonant values, cf., eqs.(10), (11). For this reason, these portions of the transition curves are omitted in Fig.3. Additional resonances will show up at higher order truncations.

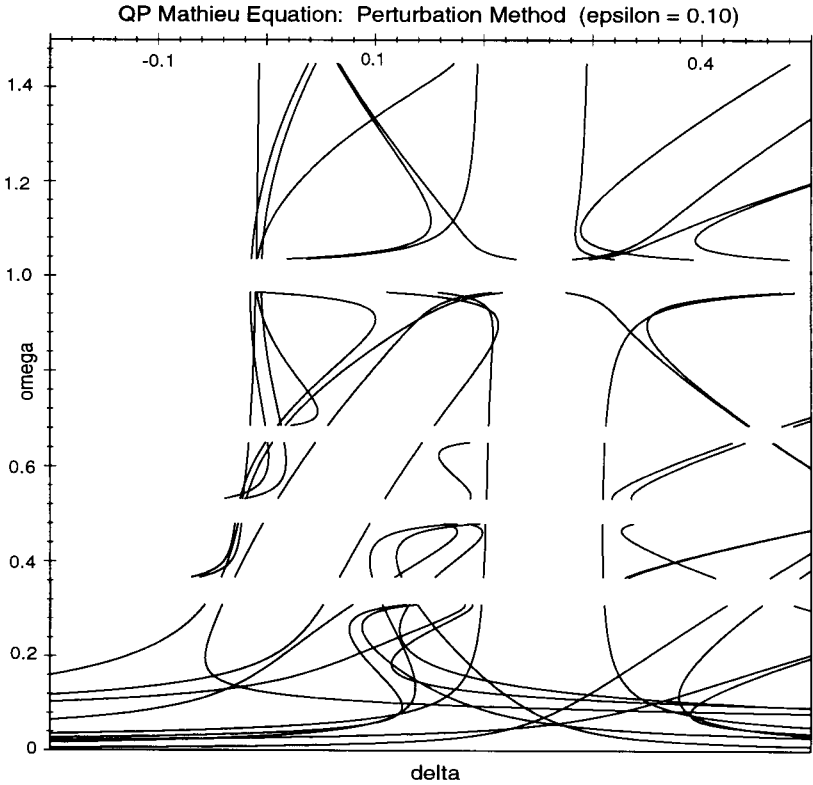


Fig.3. Transition curves of eq.(2) as determined from the perturbation method. The regions around resonant values of ω have been omitted. $\epsilon = 0.1$.

5. Harmonic Balance

Another approach which has been applied successfully to Mathieu's equation is harmonic balance [7]. This method is again based on the result from Floquet theory that along a transition curve there exist solutions with period 2π or 4π , leading to the following Fourier expansion for solutions $x(t)$:

$$x(t) = A_0 + \sum_{k=1}^{\infty} A_k \cos \frac{k}{2}t + B_k \sin \frac{k}{2}t. \quad (12)$$

Substitution of eq.(12) into eq.(1) and collecting terms (i.e., balancing harmonics) leads to an infinite set of linear, homogeneous equations for the coefficients $\{A_k, B_k\}$. For a non-trivial solution, the infinite (or Hill's) determinant of the associated coefficient matrix must vanish. By truncating this infinite system, we obtain an approximate implicit equation for the transition curves in the δ - ϵ parameter plane.

We shall apply a similar scheme to the QP Mathieu equation. The key ansatz is the generalization of the Fourier series eq.(12) to the quasiperiodic form:

$$x(t) = \sum_{n=0}^{\infty} \sum_{m=-\infty}^{\infty} A_{nm} \cos\left(\frac{n+m\omega}{2}t\right) + B_{nm} \sin\left(\frac{n+m\omega}{2}t\right). \quad (13)$$

In practice, approximate results are obtained when the infinite sums in eq.(13) are replaced by sums from 0 to N and from $-N$ to N , respectively. Since the forcing term in eq.(2) is an even function of t , the solution space can be spanned by an even solution and an odd solution. This permits us to take first B_{nm} and then A_{nm} as zero in eq.(13), thereby reducing the size of the (truncated) determinant by half. In the former case, we substitute eq.(13) with $B_{nm} = 0$ into eq.(2). Using computer algebra, we perform a trigonometric reduction and collect terms to give the following system of equations for the A_{nm} :

$$A_{n,m} \left(\delta - \frac{1}{4}(n+m\omega)^2 \right) + \frac{\epsilon}{2} (A_{n+2,m} + A_{n-2,m} + A_{n,m+2} + A_{n,m-2}) = 0. \quad (14)$$

Eqs.(14), when truncated at the N^{th} harmonic, represent $2N^2 + 2N + 1$ simultaneous equations. For example, in the case of $N = 4$, the matrix of coefficients has dimension 41, and the evaluation of the corresponding determinant and the generation of graphical plots took an hour using Maple on a Sun SPARCstation 10. As an example of the kind of results obtained by this method, see the Appendix where the determinant is displayed in factored form for the truncation $N = 2$. Figs.4 and 5 show both the sine and cosine solutions for $N = 2$ and $N = 4$, respectively. Note the absence of the small-divisor problem, in contrast to the perturbation method results of Fig.3.

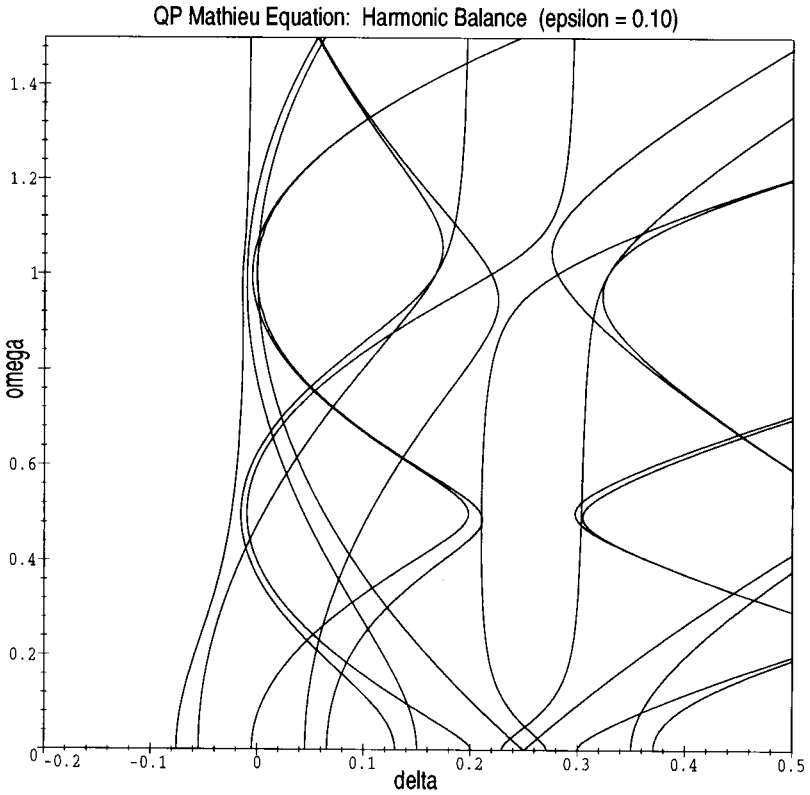


Fig.4. Transition curves of eq.(2) as determined by the method of harmonic balance for truncation order $N = 2$. $\epsilon = 0.1$.

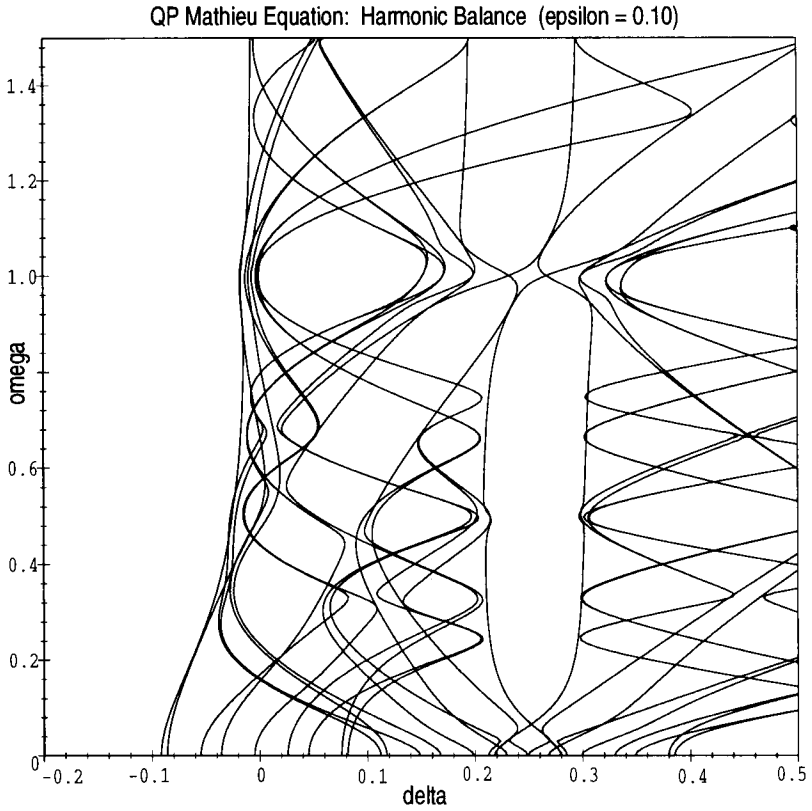


Fig.5. Transition curves of eq.(2) as determined by the method of harmonic balance for truncation order $N = 4$. $\epsilon = 0.1$.

6. Singular Perturbations

In order to better understand the nature of the dynamics of the QP Mathieu equation, we present the following singular perturbation method, valid for small values of the parameter ω . We set

$$\omega = k\epsilon \tag{15}$$

and we use the two-variable expansion method [2] in which $\xi = t$ and $\eta = \epsilon t$, whereupon eq.(2) becomes,

$$x_{\xi\xi} + 2\epsilon x_{\xi\eta} + \epsilon^2 x_{\eta\eta} + (\delta + \epsilon \cos \xi + \epsilon \cos k\eta) x = 0. \tag{16}$$

Expanding $x = x_0 + \epsilon x_1 + \dots$ and $\delta = \delta_0 + \epsilon \delta_1 + \dots$ and collecting terms, we obtain

$$x_{0\xi\xi} + \delta_0 x_0 = 0 \tag{17}$$

$$x_{1\xi\xi} + \delta_0 x_1 = -2 x_{0\xi\eta} - \delta_1 x_0 - (\cos \xi + \cos k\eta) x_0. \tag{18}$$

Eq.(17) has the solution

$$x_0 = R \cos(\sqrt{\delta_0}\xi + \theta), \tag{19}$$

where R and θ are functions of the slow time, η . Substituting eq.(19) into eq.(18), we obtain

$$\begin{aligned} x_{1\xi\xi} + \delta_0 x_1 = & 2 \sqrt{\delta_0} \left[\frac{dR}{d\eta} \sin(\sqrt{\delta_0}\xi + \theta) + R \frac{d\theta}{d\eta} \cos(\sqrt{\delta_0}\xi + \theta) \right] \\ & - \delta_1 R \cos(\sqrt{\delta_0}\xi + \theta) - R \cos k\eta \cos(\sqrt{\delta_0}\xi + \theta) \\ & - \frac{R}{2} [\cos((\sqrt{\delta_0} + 1)\xi + \theta) + \cos((\sqrt{\delta_0} - 1)\xi + \theta)]. \end{aligned} \tag{20}$$

Removal of secular terms dictates that we set to zero the coefficients of $\sin(\sqrt{\delta_0}\xi + \theta)$ and $\cos(\sqrt{\delta_0}\xi + \theta)$, giving

$$\frac{dR}{d\eta} = 0, \quad 2 \sqrt{\delta_0} R \frac{d\theta}{d\eta} - \delta_1 R - R \cos k\eta = 0. \tag{21}$$

The equation $\frac{dR}{d\eta} = 0$ means R is constant and no instability can occur. However, if δ_0 is assigned the resonant value of $\frac{1}{4}$, the term $\cos((\sqrt{\delta_0} - 1)\xi + \theta)$ in eq.(20) becomes secular:

$$\begin{aligned} \cos((\sqrt{\delta_0} - 1)\xi + \theta) &= \cos\left(\frac{\xi}{2} - \theta\right) \\ &= \cos\left(\frac{\xi}{2} + \theta - 2\theta\right) \\ &= \cos\left(\frac{\xi}{2} + \theta\right) \cos 2\theta + \sin\left(\frac{\xi}{2} + \theta\right) \sin 2\theta. \end{aligned} \tag{22}$$

This results in the appearance of some additional resonant terms in the slow-flow (21):

$$\frac{dR}{d\eta} - \frac{R}{2} \sin 2\theta = 0, \quad R \frac{d\theta}{d\eta} - \delta_1 R - R \cos k\eta - \frac{R}{2} \cos 2\theta = 0. \quad (23)$$

The first of eqs.(23) can be solved in closed form,

$$R = C e^{\frac{1}{2} \int \sin 2\theta \, d\eta}, \quad (24)$$

where C is an arbitrary constant. Eq.(24) gives R as a function of θ , and θ itself is determined by the second of eqs.(23), i.e., by

$$\frac{d\theta}{d\eta} = \delta_1 + \frac{1}{2} \cos 2\theta + \cos k\eta. \quad (25)$$

Although the R and θ variables are therefore uncoupled, the boundedness of x_0 is governed by the behavior of $R(\eta)$, cf., eq.(19). We are therefore interested in how the behavior of θ , determined by eq.(25), influences the boundedness of R via eq.(24).

The answer is this: If eq.(25) exhibits a limit cycle on the $\theta - \eta$ phase torus, then R is an exponential function of η and the x_0 motion is unstable. This follows because if $\theta(\eta)$ is a periodic function mod $n\pi$, then so is $\sin 2\theta$, but with non-zero average value taken over one orbit of the limit cycle (in general). Thus the integral in eq.(24), $\int \sin 2\theta \, d\eta$, taken over one cycle, will not in general be zero, and R will grow or decay exponentially in η . Since the Wronskian of eq.(2) is constant in t , an exponentially decaying solution must be accompanied by a second linearly independent solution which is exponentially growing. Thus a limit cycle in eq.(25) corresponds to the occurrence of an unbounded solution in eq.(2). If, on the other hand, the torus flow eq.(25) is equivalent to an irrational flow, then the integral $\int \sin 2\theta \, d\eta$ will tend to zero on the average, R will remain bounded as $t \rightarrow \infty$, and the x_0 motion will be stable.

So the question of the stability of the QP Mathieu equation (2) is reduced to the question of whether eq.(25) has a limit cycle. Unfortunately, a closed form solution of eq.(25) is unavailable. Nevertheless, we may numerically integrate eq.(25) for given values of the parameters δ_1 and k , and determine whether the phase flow exhibits a limit cycle by inspection. Before doing so, we change variables so that the phase torus is $2\pi \times 2\pi$: we set $\phi = 2\theta$ and $\tau = k\eta$, giving

$$\frac{d\phi}{d\tau} = \frac{2\delta_1 + \cos \phi + 2 \cos \tau}{k}. \quad (26)$$

Figs.6 and 7 display the phase torus of eq.(26) for parameters $(\delta_1, k) = (0.1, 0.7)$ and $(0.2, 0.7)$, respectively. Note that Fig.6 displays a flow which appears to be equivalent to an irrational flow, while Fig.7 exhibits a stable limit cycle.

The process of deciding whether a given phase portrait exhibits a limit cycle can be automated by numerically generating a Poincare map corresponding to the surface of section $\tau = \pi$. A stable limit cycle then corresponds to a stable fixed point of the associated

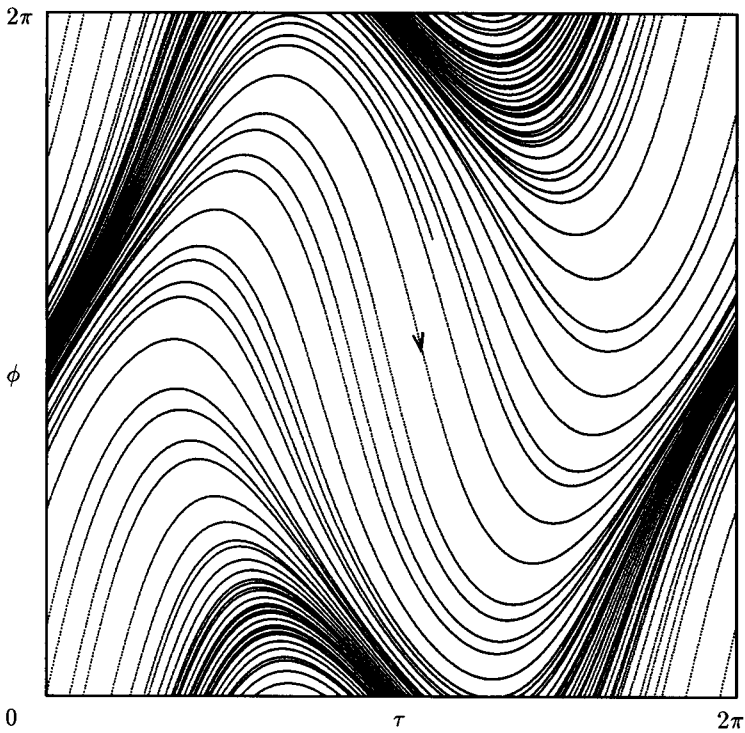


Fig.6. Numerical integration of Eq. (26) for $\delta_1 = 0.1$ and $k = 0.7$ for the initial condition $\phi = 0, \tau = 0$.

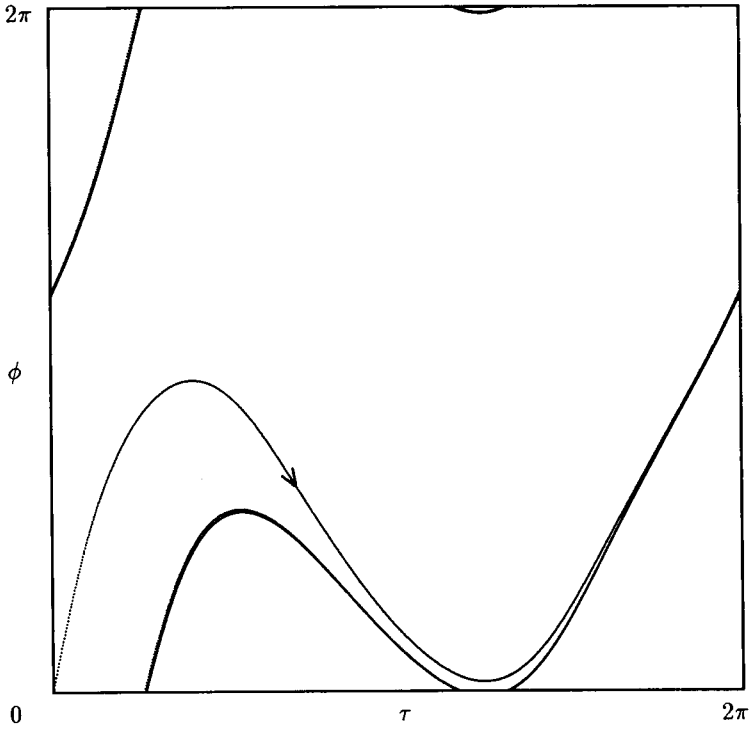


Fig.7. Numerical integration of Eq. (26) for $\delta_1 = 0.2$ and $k = 0.7$ for the initial condition $\phi = 0, \tau = 0$.

one-dimensional circle map. Fig.8 shows the result of such a procedure, in which thousands of points were chosen at random in the (δ_1, k) parameter space, and the presence of a dot represents stability, i.e., the absence of a stable limit cycle.

Fig.8 is symmetric about the k -axis. This may be shown by defining

$$\tilde{\phi} = -(\phi + \pi), \quad \tilde{\tau} = \tau + \pi, \quad \tilde{\delta}_1 = -\delta_1 \quad (27)$$

Eq.(26) is unchanged by the transformation (27),

$$\frac{d\tilde{\phi}}{d\tilde{\tau}} = \frac{2\tilde{\delta}_1 + \cos \tilde{\phi} + 2 \cos \tilde{\tau}}{k}. \quad (28)$$

But since the transformation (27) is a rigid motion (a translation and a reflection), it can't change the phase portrait. Thus the stability is unchanged when δ_1 is replaced by $-\delta_1$.

7. Conclusions

A comparison of Figs.1-5 reveals general agreement between the numerical and analytical approximations to the stability charts of the quasiperiodic Mathieu equation. The method of Lyapunov exponents in Fig.2 shows greater detail than the simple numerical integration of Fig.1, although Fig.1 involved four times more computation than Fig.2! Fig.3, based on the perturbation method, displays gaps where portions of the transition curves (which lie near the resonant values of ω) have been omitted, while Figs.4 and 5 generated by the method of harmonic balance do not suffer from this singular behavior. All four methods show that for small ϵ the two largest instability regions lie in the neighborhood of the curves $\delta = \frac{1}{4}$ and $\delta = \frac{\omega^2}{4}$, each of which represents a 2:1 resonance between the respective driving frequency (1 and ω) and the unforced frequency ($\sqrt{\delta}$). The analytical methods show that the thickness of these two instability regions is approximately ϵ . However it is evident from both the numerical plots as well as from the analytical results that there are many additional smaller instability regions. For example, the point of intersection between these two largest instability regions, namely $\delta = \frac{1}{4}, \omega = 1$, is the birthplace of a number of smaller instability regions; (see Figs.1 and 2). For this choice of parameters, both driving frequencies are in 2:1 resonance with the unforced frequency and we may expect the unfolding of such a degeneracy to be accompanied by a diversity of bifurcations.

Why is it that the perturbation method fails to give good results at points where the harmonic balance method works well? We offer the following explanation based on a simple model which is not directly related to the quasiperiodic Mathieu equation, but which we think captures the essential phenomenon. Suppose that we were interested in a perturbation solution to a problem which had the form,

$$\left(\delta - \frac{1}{4}\right)\left(\delta - \frac{\omega^2}{4}\right) = \epsilon. \quad (29)$$

This form is chosen because it is a simplified version of the kind of expression generated by the harmonic balance method. In seeking a perturbation solution we would expand δ in a power series in ϵ :

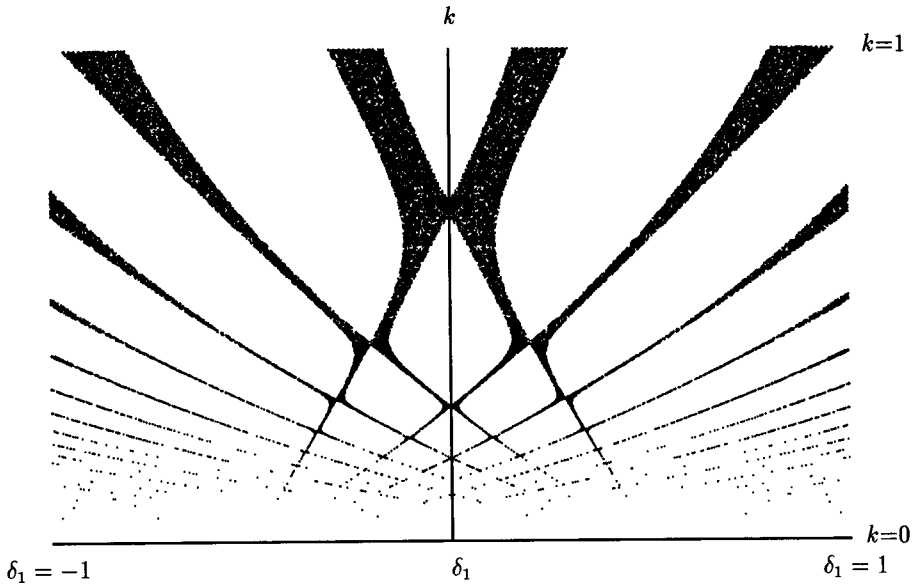


Fig.8. Stability of Eq. (2) as obtained by singular perturbation method. Eq. (26) was numerically integrated for thousands of points randomly chosen in the (δ_1, k) parameter plane. Black=no limit cycle=stable, white=limit cycle=unstable. Compare with Fig.9 where $\delta = \frac{1}{4} + \epsilon\delta_1 + \dots$, $\omega = k\epsilon$.

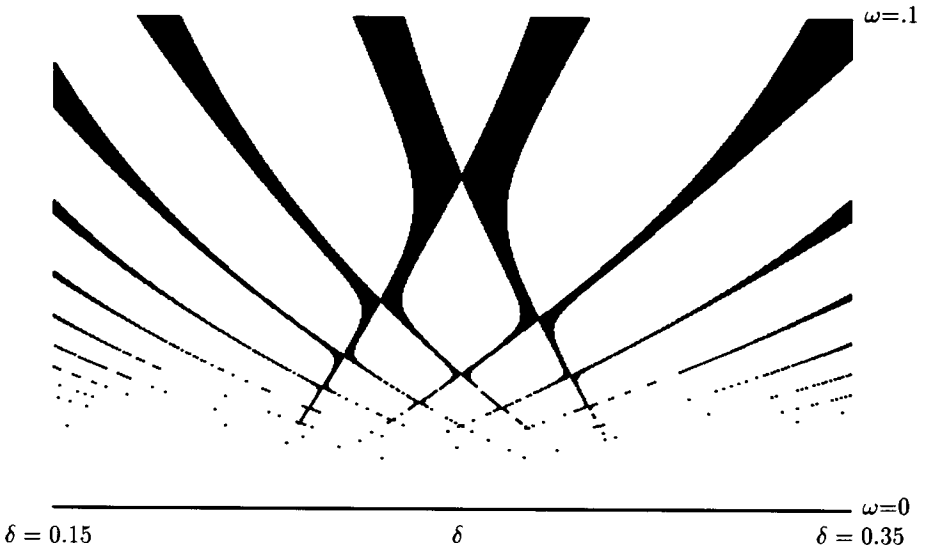


Fig.9. Stability of Eq. (2) for $\epsilon = 0.1$ as obtained by direct numerical integration. This Figure is an enlargement of a portion of Fig.1. Black=stable, white=unstable. Compare with Fig.8.

$$\delta = \delta_0 + \epsilon\delta_1 + \dots \tag{30}$$

Substituting eq.(30) into eq.(29) and collecting terms gives the perturbation expansion:

$$\delta = \frac{1}{4} + \frac{4}{1 - \omega^2}\epsilon + \dots \tag{31}$$

Note that eq.(31) is singular at $\omega^2 = 1$, in a manner similar to the misbehavior of the perturbation solutions of the quasiperiodic Mathieu equation, cf., eqs.(10), (11). We may say that the reason the perturbation method failed is that the assumed form of the solution, eq.(30), is inappropriate. By contrast, the implicit form of eq.(29), which is analogous to the results of the harmonic balance method, has no small-divisor difficulty.

Why does the harmonic balance method work? We offer an explanation based on restricting ω to rational values: $\omega = p/q$ where p and q are relatively prime positive integers. We may justify this restriction by noting that any irrational number can be approximated by a rational to any degree of accuracy. With this restriction, the QP Mathieu equation becomes the following Hill's equation:

$$\ddot{x} + (\delta + \epsilon \cos t + \epsilon \cos \frac{p}{q}t) x = 0. \tag{32}$$

Assuming $\omega < 1$, the term $\epsilon \cos t + \epsilon \cos \frac{p}{q}t$ has period $T = 2\pi q$. According to Floquet theory, any solution $x(t)$ along the transition curves of equation (32) has minimum period T or $2T$, and hence, can be expanded in a Fourier series:

$$x(t) = A_0 + \sum_{k=1}^{\infty} A_k \cos \frac{k}{2q}t + B_k \sin \frac{k}{2q}t. \tag{33}$$

Since p and q are relatively prime, any integer k can be expressed as the linear combination $k = nq + mp$ for some $n, m \in \mathbf{Z}$ [4]. As a result, the set of integers can be put into a one-to-one correspondence with the following set of ordered pairs of integers:

$$\mathcal{M} = \{(n, m) \in \mathbf{Z} \times \mathbf{Z} : k = nq + mp, k \in \mathbf{Z}\}. \tag{34}$$

Ordered pairs that yield the same integer are identified and defined to be in the same equivalence class. Hence, the correspondence is actually between \mathbf{Z} and the set of equivalence classes. The Fourier series (33) for $x(t)$ can then be expressed as follows:

$$\begin{aligned} x(t) &= \sum_{\mathcal{M}} A_{nm} \cos \frac{nq + mp}{2q}t + B_{nm} \sin \frac{nq + mp}{2q}t \\ &= \sum_{\mathcal{M}} A_{nm} \cos \frac{n + m\omega}{2}t + B_{nm} \sin \frac{n + m\omega}{2}t, \end{aligned}$$

which is in the form of the ansatz given by eq.(13).

We also presented a singular perturbation method which is valid for small ω , in the neighborhood of $\delta = \frac{1}{4}$. The criterion for stability was the presence of an irrational torus flow in eq.(26), (cf., Fig.8). These results may be compared with those obtained by numerical integration by enlarging the region around $\delta = \frac{1}{4}$ in Fig.1, as shown in Fig.9. We note that there is excellent agreement between the perturbation results of Fig.8 and the direct numerical treatment of Fig.9.

8. References

1. Abel, J.M., 1970, "On an Almost Periodic Mathieu Equation", *Quart.Appl.Math.* vol.28, pp.205-217.
2. Bender, C.M. and Orszag, S.A., 1978, *Advanced Mathematical Methods for Scientists and Engineers*, McGraw-Hill, New York.
3. Davis, S.H. and Rosenblat, S., 1980, "A quasiperiodic Mathieu-Hill equation", *SIAM J.Appl.Math.* vol.38, pp.139-155.
4. Herstein, I.N., 1975, *Topics In Algebra, 2nd Edition*, Wiley, New York.
5. Rand, R. and Hastings, R., 1995, "A Quasiperiodic Mathieu Equation", Proceedings of the 1995 Design Engineering Technical Conferences, Boston, Massachusetts, Sept.17-20, 1995, Vol. 3, Part A: *Vibration of Nonlinear, Random and Time-Varying Systems*, vol.DE-Vol.84-1, pp.747-758, American Soc. Mech. Engineers.
6. Rand, R.H., 1994, *Topics in Nonlinear Dynamics with Computer Algebra*, Gordon and Breach, Langhorne, PA.
7. Stoker, J.J., 1950, *Nonlinear Vibrations in Mechanical and Electrical Systems*, Wiley, New York.
8. Vrscaj, E.A., 1991, "Irregular behavior arising from quasiperiodic forcing of simple quantum systems: insight from perturbation theory", *J.Phys.A:Math.Gen.* vol.24, pp.L463-L468.
9. Zounes, R.S. and Rand, R.H., 1996, "Transition Curves in the Quasiperiodic Mathieu Equation", in *Nonlinear Dynamics and Controls*, editors:A.K.Bajaj, N.Sri Namachchivaya, and M.A.Franckek, ASME Book No.G01025, pp.1-6, American Soc. Mech. Engineers.
10. Zounes, R.S., 1997, "Analytic Techniques for the Investigation of Asymptotic Properties of the Quasiperiodic Mathieu Equation", Ph.D. thesis, Center for Applied Mathematics, Cornell University.

9. Appendix

We present below the results of the harmonic balance method for truncation $N = 2$.

sine-series solution:

$$\begin{aligned} \det = 0 = & -64(-\omega^2 + 2\omega + 4\delta - 1)(4\delta - 1 - 2\omega - \omega^2) \\ & (8\epsilon^3 + (-12\omega^2 + 48\delta - 32)\epsilon^2 + (-16\omega^2 + 2\omega^4 + 32 + 32\delta^2 - 64\delta - 16\omega^2\delta)\epsilon \\ & + 16\omega^2 + \omega^6 + 128\delta^2 - 64\delta - 64\delta^3 - 12\omega^4\delta + 48\omega^2\delta^2 - 8\omega^4) \\ & (8\epsilon^3 + (48\delta - 32\omega^2 - 12)\epsilon^2 + (-16\omega^2 + 32\delta^2 - 64\omega^2\delta - 16\delta + 2 + 32\omega^4)\epsilon \\ & - 8\omega^2 + 1 - 64\omega^4\delta + 48\delta^2 + 16\omega^4 - 64\delta^3 + 128\omega^2\delta^2 - 12\delta) \\ & (\epsilon^4 + (-4\omega^2 + 6\delta - 2 - 4\delta^2 - 2\omega^4 + 6\omega^2\delta)\epsilon^2 \\ & + 4\omega^2 + 12\omega^2\delta^2 - 8\omega^4 - 4\omega^6\delta + 12\omega^4\delta^2 - 12\delta^3\omega^2 \\ & + 4\omega^6 - 4\omega^2\delta + 12\delta^2 - 12\delta^3 - 4\delta - 4\omega^4\delta + 4\delta^4) \end{aligned}$$

cosine-series solution:

$$\begin{aligned} \det = 0 = & 512(-16\epsilon^2 - 2\omega^2 + 1 - 8\delta - 8\omega^2\delta + 16\delta^2 + \omega^4) \\ & (8\epsilon^3 + (32\omega^2 - 48\delta + 12)\epsilon^2 + (-16\omega^2 + 32\delta^2 - 64\omega^2\delta - 16\delta + 2 + 32\omega^4)\epsilon \\ & + 64\omega^4\delta - 48\delta^2 - 16\omega^4 - 128\omega^2\delta^2 - 1 + 64\delta^3 + 8\omega^2 + 12\delta) \\ & (-8\epsilon^3 + (-12\omega^2 + 48\delta - 32)\epsilon^2 + (16\omega^2 - 32 + 16\omega^2\delta + 64\delta - 2\omega^4 - 32\delta^2)\epsilon \\ & - 12\omega^4\delta + 128\delta^2 - 8\omega^4 + 48\omega^2\delta^2 - 64\delta - 64\delta^3 + 16\omega^2 + \omega^6) \\ & ((5\omega^4\delta - 1 + 4\delta^3 - 8\omega^2\delta^2 + \omega^2 + \omega^4 + 5\delta - \omega^6 + 2\omega^2\delta - 8\delta^2)\epsilon^2 \\ & + 2\omega^6\delta^2 + 2\delta^2 - 2\omega^2\delta + 4\omega^4\delta + 6\delta^4\omega^2 - 6\delta^3 - 2\omega^6\delta \\ & + 2\omega^2\delta^2 - 6\delta^3\omega^2 + 6\delta^4 - 2\delta^5 - 6\omega^4\delta^3 + 2\omega^4\delta^2) \end{aligned}$$